

The Linear Wave Response of a Periodic Array of Floating Elastic Plates

C. D. Wang (cynthiaw@quakes.uq.edu.au)

Institute of Information and Mathematical Sciences, Massey University, Auckland, New Zealand. Current address: Earth Systems Science Computational Centre, Australian Computational Earth Systems Simulator, The University of Queensland, Brisbane QLD 4072 Australia

M. H. Meylan (meylan@math.auckland.ac.nz)

Department of Mathematics, University of Auckland, Private Bag 92019, Auckland, New Zealand.

R. Porter (richard.porter@bristol.ac.uk)

School of Mathematics, University of Bristol, Bristol, BS8 1TW, UK.

Abstract. The problem of an infinite periodic array of identical floating elastic plates subject to forcing from plane incident waves is considered. This study is motivated by the problem of trying to model wave propagation in the marginal ice zone, a region of ocean consisting of an arbitrary packing of floating ice sheets. It is shown that the problem considered can be formulated exactly in terms of the solution to an integral equation in a manner similar to that used for the problem of wave scattering by a single elastic floating plate, the key difference here being the use of a modified periodic Green function. The convergence of this Green function in its original form is poor, but can be accelerated by a transformation. It is shown that the results from the method satisfy energy conservation and that in the particular case of a fixed rigid rectangular plate which spans the periodicity uniformly the solution reduces to that for a two-dimensional rigid dock. We also present solutions for a range of elastic plate geometries.

Keywords: Ice sheet, elastic plates, periodic Green function, water waves

1. Introduction

The thin elastic plate of shallow draft floating on the surface of water can be used to model a range of physical systems, for example ice floes or so-called very large floating structures, which are of particular interest in proposals to build offshore floating runways. It is also of theoretical importance as one of the simplest models of hydroelasticity. It is not surprising therefore that the floating elastic plate has been the subject of a significant body of research. Much of this research, especially that which was motivated by the construction of very large floating structures, is summarised in the review papers by (Kashiwagi, 2000) and (Watanabe et al., 2004). The review paper by (Squire et al.,



© 2004 Kluwer Academic Publishers. Printed in the Netherlands.

1995) summarises the research prior to 1995 which was motivated by modelling sea ice floes, but does not include the more recent work, (Meylan and Squire, 1996) and (Meylan, 2002), in which the solution for wave scattering by a three-dimensional ice floe is presented.

Our aim here is to present a method of solution to the problem of wave scattering by an infinite periodic array of floating elastic plates. This study is motivated by trying to further the understanding of the problem of wave scattering in the marginal ice zone. The marginal ice zone consists of a vast field of broken ice floes each of which have a thickness (typically $\approx 1\text{-}2\text{m}$) much smaller than the typical horizontal lengthscale of the floe, or of the wavelength of waves supported by the floe, and it is usual to model the ice floe as a thin elastic plate. These ice floes are subject to intense wave forces whose source originates from the open ocean. On account of the fact that that the floes are themselves able to support wave propagation, wave energy is capable of travelling large distances within the marginal ice zone where it can assist ice breakup.

Previous work aimed at trying to model wave interaction by isolated three-dimensional regular and irregular ice floes has been performed in (Meylan and Squire, 1996) and (Meylan, 2002), respectively. For more complicated arrangements involving an arbitrary, but finite, number of irregular ice floes see (Peter & Meylan 2004) although the number of floes that can be dealt with is limited by numerical considerations. Although this latter work includes the effect of interaction between neighbouring ice floes, it does not allow one to capture the effects of a plane wave incident upon a large linear array of ice floes. One method of overcoming this, which also allows significant analytic progress to be made is to consider wave scattering by an infinite periodic array of identical ice floes, being irregular in shape. Of course ice fields are not periodic, but this arrangement does provide some information especially if some kind of statistical averaging of the results over the floe geometries and spacings is performed. Furthermore, the solution readily lends itself to a wide-spacing method similar to that used by (Evans, 1995) which allows accurate approximations to wave scattering by multiple rows of non-identical ice floes. Central to such a procedure is knowledge of the scattering process for each row in isolation.

The problem of determining the scattering of waves by periodic arrays of obstacles subject to wave forcing has received considerable research attention and spans a broad range of physical disciplines including solid-state physics, acoustics, optics, etc. In many applications, the interest centres on arrangements which are periodic in two directions (for example, the study of crystallography). In the present context of water wave propagation and its interaction with flexible

surface structures, (Chou, 1998) has investigated the effect of an infinite doubly-periodic array of elastic plates on wave propagation. In the modelling of the plate equations, Chou incorporates both bending stiffness and tension effects, so that the discussion of the results not only includes the case of pure bending of elastic plates in the absence of compression forces (as considered here), but also, by setting the stiffness to zero, pure tensional effects which would describe, for example, periodic arrays of taught membranes. However, in contrast to the work described here, the doubly-periodic configuration allows significant simplification in the solution procedure by applying Floquet's theorem to reduce the problem to one on a finite domain with periodic boundary conditions. Moreover, problems involving infinite doubly-periodic structures only offer information about the possibility of wave propagation throughout the array (in the form of so-called pass-bands or stop-bands) and cannot address the diffraction of plane waves from infinity.

For arrays which are periodic in one direction only, the situation is different and diffraction grating effects occur. Thus, for an incident plane wave of a particular given wave frequency, a finite number of distinct plane waves propagating away from the array at certain discrete angles will occur. In the context of water waves and fixed periodic arrays, (Twersky, 1952) was able to solve the problem of a periodic array of vertical circular cylinders. The uniformity of the configuration in the depth coordinate implies that the resulting equations also describe two-dimensional acoustic wave scattering, in this case by circular cylinders. The problem of (Twersky, 1952), who used Schlömilch series to sum slowly-convergent series involving Hankel functions, was re-considered by (Linton and Evans, 1993) who used a so-called multipole method. For periodic arrays of rectangular cylinders extending uniformly through the depth, (Ferryhough and Evans, 1995), used domain decomposition and mode matching to derive an integral equation formulation to the problem. In order to consider more general cylinder profiles, boundary integral methods are inevitable and require the use of a periodic Green function. In its most basic form, the Green function consists of a series involving Hankel functions which is slowly convergent and unsuitable for numerical computation. Hence (Linton, 1998) compared a number of different representations of the periodic Green function, designed to increase the convergence characteristics. (Evans, 1999) used the work of (Linton, 1998) to compute so-called Rayleigh-Bloch waves (or trapped waves) along a periodic array of cylinders of arbitrary cross-section. A number of papers in recent years have concentrated on similar ideas, to those of (Evans, 1999), a primary motivation being the connection between large wave responses in large

finite arrays of cylinders and the trapped waves in infinite periodic arrays (see (Maniar and Newman, 1997)).

In contrast to the body of work cited in the previous paragraph, the present work differs significantly in two respects. First, the problem involving periodic elastic plates on the water surface implies that the problem is fully three-dimensional. Secondly, the scattering obstacles are neither fixed (as above) nor rigid, but are in fact themselves capable of supporting wave motions. Thus the coupling between the plate motion and the motion of the water adds an extra degree of complication to the problem.

The outline of the paper is as follows. In section 2 the non-dimensional small-amplitude equations for time-harmonic motion are formulated. In section 3, an integral equation is derived connecting the motion of the plate to that of the water. In doing so the periodic Green function is defined in terms of the three-dimensional free-surface Green function. In section 4, a variational principle for the motion of the plate is defined and a Rayleigh-Ritz approximation is used to reduce it to a linear system of equations. The same approximation is used in the integral equation to provide a second set of linear equations coupling the motion of the plate to the water. Section 5 concentrates on improving the otherwise slow convergence of the periodic Green function and section 6 describes how the far-field reflected and transmitted waves are calculated from the integral formulation. Finally, in section 7 a range of numerical results are presented and discussed and the work is concluded in section 8.

2. Problem Formulation: An Infinite Array of Elastic Plates

We begin by formulating the problem. Cartesian coordinates (x, y, z) are chosen with z vertically upwards such that $z = 0$ coincides with the mean free surface of the water. An infinite array of identical thin elastic plates float on the surface of the water, periodically spaced along the y -axis with uniform separation l . The problem is to determine the motion of the water and the plates when plane waves are obliquely-incident from $x = -\infty$ upon the periodic array of plates.

The plates are assumed to be of zero draft and occupy $\mathbf{x} \in \Delta_m$, $-\infty < m < \infty$ on $z = 0$ where $\mathbf{x} = (x, y)$ represents the Cartesian vector lying in the mean free surface. The plates are assumed to have arbitrary shape, and periodicity implies that if $\mathbf{x} \in \Delta_0$, then $\mathbf{x}_m = (x, y + ml) \in \Delta_m$, $-\infty < m < \infty$. This array of plates is shown in Figure 1.

2.1. ELASTIC PLATE EQUATIONS

The equation of motion for the plate elevation $W(x, y, t)$, where t is time, is given by the thin elastic plate (or Kirchhoff) equation,

$$D\nabla_h^4 W + \rho_i h \frac{\partial^2 W}{\partial t^2} = p, \quad (1)$$

(Timoshenko and Woinowsky-Krieger, 1959) where D is the flexural rigidity, ρ_i is the density, and h the uniform thickness of the elastic plate. Here, p is the excess pressure (i.e. excluding atmospheric pressure and the weight of the plate) exerted by the fluid and ∇_h^2 is the two-dimensional horizontal Laplacian in the plane $z = 0$ (we shall reserve ∇^2 to mean the three-dimensional Laplacian). In addition, on the free edges of the plates, $\mathbf{x} \in \partial\Delta_m$, boundary conditions expressing the vanishing of bending moment and shearing stress apply, which are written as

$$\left[\nabla_h^2 - (1 - \nu) \left(\frac{\partial^2}{\partial s^2} + \kappa(s) \frac{\partial}{\partial n} \right) \right] W = 0, \quad (2)$$

$$\left[\frac{\partial}{\partial n} \nabla_h^2 + (1 - \nu) \frac{\partial}{\partial s} \left(\frac{\partial}{\partial n} \frac{\partial}{\partial s} - \kappa(s) \frac{\partial}{\partial s} \right) \right] W = 0, \quad (3)$$

where ν is Poisson's ratio and

$$\nabla_h^2 = \frac{\partial^2}{\partial x^2} + \frac{\partial^2}{\partial y^2} = \frac{\partial^2}{\partial n^2} + \frac{\partial^2}{\partial s^2} + \kappa(s) \frac{\partial}{\partial n}.$$

Here, $\kappa(s)$ is the curvature of the boundary, $\partial\Delta_m$, as a function of arclength s along $\partial\Delta_m$; $\partial/\partial s$ and $\partial/\partial n$ represent derivatives tangential and normal to the boundary $\partial\Delta_m$.

Equations (2) and (3) can be established from (Porter and Porter, 2004) who considered the more complicated case of a plate of varying thickness and derived the edge conditions from a variational principle similar to the one used later in this paper. A direct derivation of the edge conditions from the underlying constitutive equations for a thin elastic plate can found elsewhere, for example (de Veubeke, 1979). We remark that in the case where the boundary of the elastic plates is piecewise linear, such that $\kappa(s) = 0$, the equations above reduce to the simpler form

$$\left(\frac{\partial^2}{\partial n^2} + \nu \frac{\partial^2}{\partial s^2} \right) W = 0$$

and

$$\left(\frac{\partial^3}{\partial n^3} + (2 - \nu) \frac{\partial^3}{\partial n \partial s^2} \right) W = 0.$$

2.2. EQUATIONS OF MOTION FOR THE WATER

We consider water of infinite depth. Under the usual assumptions of small-amplitude waves above an incompressible and irrotational fluid, there exists a velocity potential $\Phi(x, y, z, t)$ satisfying Laplace's equation together with the appropriate linearised boundary conditions, namely

$$\left. \begin{aligned} \nabla^2 \Phi &= 0, & -\infty < z < 0, \\ \Phi, |\nabla \Phi| &\rightarrow 0, & z \rightarrow -\infty, \\ \frac{\partial \Phi}{\partial z} &= \frac{\partial W}{\partial t}, & z = 0, \\ -\rho \frac{\partial \Phi}{\partial t} - \rho g W &= p, & z = 0, \end{aligned} \right\} \quad (4)$$

where the pressure, p , has already been introduced in (1), ρ is the water density, and g is gravitational acceleration. W is the time-dependent displacement of the plate when $\mathbf{x} \in \Delta_m$. When $\mathbf{x} \notin \Delta_m$, we take $p = 0$ in the above and now W represents the elevation of the water surface. In addition to (4), radiation conditions at infinity need to be applied and these will formally be introduced later.

2.3. NON-DIMENSIONALISING THE VARIABLES

We non-dimensionalise the spatial variables with respect to a length parameter L (for example, L may be derived from the area of the plate or L may be the characteristic length $(D/\rho g)^{1/4}$) and the time variables with respect to $\sqrt{L/g}$. The dimensionless variables are therefore given by

$$(\bar{x}, \bar{y}, \bar{z}, \bar{W}) = \frac{1}{L}(x, y, z, W), \quad \bar{t} = t\sqrt{\frac{g}{L}}, \quad \bar{p} = \frac{p}{\rho g L} \quad \text{and} \quad \bar{\Phi} = \frac{\Phi}{L\sqrt{Lg}}.$$

Using the dimensionless variables equation (1) combined with the last equation of (4) becomes

$$\beta \bar{\nabla}_h^4 \bar{W} + \gamma \frac{\partial^2 \bar{W}}{\partial \bar{t}^2} = \bar{p} = - \left. \frac{\partial \bar{\Phi}}{\partial \bar{t}} \right|_{\bar{z}=0} - \bar{W}, \quad (5)$$

where the dimensionless parameters associated with the motion of the plate, β and γ , representing the 'stiffness' and 'mass loading' of the plate respectively, are given by

$$\beta = \frac{D}{\rho g L^4} \quad \text{and} \quad \gamma = \frac{\rho_i h}{\rho L}.$$

This notation is based on (Tayler, 1986).

Hereafter, we will work with dimensionless variables only but omit the overbar from all variables for reasons of clarity. Note that from now on we will use l to mean the non-dimensional floe separation $\bar{l} = l/L$.

2.4. THE SINGLE FREQUENCY EQUATIONS

We will consider the solution for a single frequency and we can therefore represent the displacement and the potential as the real parts of complex functions in which the time dependence is $e^{-i\omega t}$ where ω is the dimensionless radian frequency, i.e.

$$\begin{aligned} W(x, y, t) &= \operatorname{Re} \left[\left(\frac{i}{\omega} \right) w(x, y) e^{-i\omega t} \right], \\ \Phi(x, y, z, t) &= \operatorname{Re} \left[\phi(x, y, z) e^{-i\omega t} \right], \end{aligned}$$

where we have introduced an additional scaling for W to simplify the equations which follow.

Therefore equation (5) becomes

$$\beta \nabla_h^4 w(x, y) + (1 - \omega^2 \gamma) w(x, y) = \omega^2 \phi(x, y, 0). \quad (6)$$

Combining the non-dimensionalisation with the time assumption we also have from (4)

$$\frac{\partial \phi}{\partial z} = w, \quad z = 0 \quad (7)$$

with

$$\left. \begin{aligned} \nabla^2 \phi &= 0, & -\infty < z < 0, \\ \phi, |\nabla \phi| &\rightarrow 0, & z \rightarrow -\infty, \end{aligned} \right\} \quad (8)$$

For $\mathbf{x} \notin \Delta_m$, (6) still holds, but with $\beta = \gamma = 0$ and combining with (7) gives the usual free-surface condition

$$\frac{\partial \phi}{\partial z} - k\phi = 0, \quad \text{on } z = 0, \quad \text{where } k = \omega^2$$

and k is the dimensionless wavenumber (i.e. the dimensionless wavelength is $\lambda = 2\pi/k$). The velocity potential also satisfies the Sommerfeld radiation condition as $|\mathbf{x}| \rightarrow \infty$,

$$\lim_{|\mathbf{x}| \rightarrow \infty} \sqrt{|\mathbf{x}|} \left(\frac{\partial}{\partial |\mathbf{x}|} - ik \right) (\phi - \phi^{\text{in}}) = 0, \quad (9)$$

((Wehausen and Laitone, 1960)). In equation (9), ϕ^{in} is the incident wave potential given by

$$\phi^{\text{in}} = \frac{A}{k} e^{ik(x \cos \theta + y \sin \theta)} e^{kz}, \quad (10)$$

where A is the dimensionless amplitude and θ is the direction of propagation of the wave.

3. Transformation to an Integral Equation

We now apply Floquet's theorem, which states that potential and the displacement from adjacent plates differ only by a phase factor (Scott, 1998). If the potential under the *central* plate Δ_0 is given by $\phi(\mathbf{x}_0, 0)$, $\mathbf{x}_0 \in \Delta_0$, then by Floquet's theorem the potential satisfies

$$\phi(\mathbf{x}_m, 0) = \phi(\mathbf{x}_0, 0)e^{im\sigma t}, \quad (11)$$

and the displacement of the plate Δ_m satisfies

$$w(\mathbf{x}_m) = w(\mathbf{x}_0)e^{im\sigma t}, \quad (12)$$

where $\mathbf{x}_m \in \Delta_m$, $-\infty < m < \infty$ and the phase difference is $\sigma = k \sin \theta$ (see, for example, (Linton, 1998)).

A standard approach to the solution of the equations of motion for the water (6), (7), (8) is to transform these equations into a boundary integral equation using the free-surface Green function for infinite depth (see (Wehausen and Laitone, 1960; Kim, 1965)). In doing so we obtain

$$\phi(\mathbf{x}, 0) = \phi^{\text{in}}(\mathbf{x}, 0) + \sum_{m=-\infty}^{\infty} \int_{\Delta_m} G(\mathbf{x}, 0; \boldsymbol{\xi}) [k\phi(\boldsymbol{\xi}, 0) - w(\boldsymbol{\xi})] d\boldsymbol{\xi} \quad (13)$$

where $\boldsymbol{\xi} = (\xi, \eta)$ and $G(\mathbf{x}, z; \boldsymbol{\xi})$ is the free-surface Green function satisfying

$$\left. \begin{aligned} \nabla^2 G &= 0, & -\infty < z < 0, \\ \frac{\partial G}{\partial z} - kG &= -\delta(\mathbf{x} - \boldsymbol{\xi}), & z = 0, \\ G, |\nabla G| &\rightarrow 0, & z \rightarrow -\infty. \end{aligned} \right\} \quad (14)$$

which, on $z = 0$, is given by

$$G(\mathbf{x}, 0; \boldsymbol{\xi}) = -\frac{1}{4\pi} \left(\frac{2}{|\mathbf{x} - \boldsymbol{\xi}|} - \pi k \left[\mathbf{H}_0(k|\mathbf{x} - \boldsymbol{\xi}|) + Y_0(k|\mathbf{x} - \boldsymbol{\xi}|) - 2i\pi J_0(k|\mathbf{x} - \boldsymbol{\xi}|) \right] \right), \quad (15)$$

In the above \mathbf{H}_0 is the Struve function of order zero, J_0 is the Bessel function of the first kind of order zero and Y_0 is the Bessel function of the second kind of order zero (Abramowitz and Stegun, 1970).

Using (11) and (12) in (13) we obtain

$$\begin{aligned} \phi(\mathbf{x}, 0) &= \phi^{\text{in}}(\mathbf{x}, 0) \\ &+ \sum_{m=-\infty}^{\infty} \int_{\Delta_0} G(\mathbf{x}, 0; \boldsymbol{\xi} + (0, m)) [k\phi(\boldsymbol{\xi}, 0) - w(\boldsymbol{\xi})] e^{im\sigma l} d\boldsymbol{\xi} \end{aligned}$$

which can be written alternatively as

$$\phi(\mathbf{x}, 0) = \phi^{\text{in}}(\mathbf{x}, 0) + \int_{\Delta_0} G_{\mathbf{P}}(\mathbf{x}; \boldsymbol{\xi}) [k\phi(\boldsymbol{\xi}, 0) - w(\boldsymbol{\xi})] d\boldsymbol{\xi}, \quad (16)$$

where the kernel $G_{\mathbf{P}}$ (referred to as the *periodic Green function*) is given by

$$G_{\mathbf{P}}(\mathbf{x}; \boldsymbol{\xi}) = \sum_{m=-\infty}^{\infty} G(\mathbf{x}, 0; \boldsymbol{\xi} + (0, m)) e^{im\sigma l}. \quad (17)$$

4. Solution of the Integral Equation

The integral equation (16) is identical to the integral equation for a single plate (see (Meylan, 2002)) except for the modification to the Green function. Furthermore, the periodic Green function $G_{\mathbf{P}}$ has the same singularity at $\mathbf{x} = \boldsymbol{\xi}$ as the standard free-surface Green function G . We solve equation (16) using a higher-order method, which is explained in detail in (Wang and Meylan, 2004). We will briefly outline the solution method here.

We expand the plate potential and displacement as

$$\left. \begin{aligned} w(\mathbf{x}) &\approx \sum_{i=1}^{3q} w_i \chi_i(\mathbf{x}) = \vec{\chi}^T(\mathbf{x}) \vec{w} \\ \phi(\mathbf{x}, 0) &\approx \sum_{i=1}^{3q} \phi_i \chi_i(\mathbf{x}) = \vec{\chi}^T(\mathbf{x}) \vec{\phi} \end{aligned} \right\} \quad (18)$$

where \vec{w} and $\vec{\phi}$ are vectors representing the values of the displacement and potential, respectively, and their horizontal derivatives at the q nodes, and $\vec{\chi}$ is a vector of the associated basis functions. We can express $\vec{\chi}^T(\mathbf{x})$ in terms of the non-conforming basis functions for each square panel, denoted by $\mathbf{N}_d(\mathbf{x})$, ((Petyt, 1990; Wang and Meylan, 2004) as

$$\vec{\chi}^T(\mathbf{x}) = \left(\sum_{d=1}^N \mathbf{N}_d(\mathbf{x}) [o]_d \right) \quad (19)$$

where N is the number of panels and the matrix $[o]_d$ is the *assembler matrix*. Both $\mathbf{N}_d(\mathbf{x})$ (which is a 1×12 matrix) and $[o]_d$ (which is a $12 \times 3q$ matrix) are discussed in detail in (Wang and Meylan, 2004).

The equation governing the motion of the plate (6) and the time-harmonic non-dimensionalised versions of the boundary conditions at the edge of the plate (2), (3) are equivalent to the variational principle (Porter and Porter, 2004; Hildebrand, 1965; Meylan, 2001), $\delta L = 0$ where

$$L(w) = \frac{1}{2} \int_{\Delta_0} \beta \left[\left(\nabla_h^2 w \right)^2 - 2(1 - \nu) \left(\frac{\partial^2 w}{\partial x^2} \frac{\partial^2 w}{\partial y^2} - \left(\frac{\partial^2 w}{\partial x \partial y} \right)^2 \right) \right] + (1 - k\gamma) w^2 - 2kw\phi|_{z=0} d\mathbf{x}. \quad (20)$$

The three terms in the integrand above represent, respectively, the strain energy of the plate, the acceleration, and the dynamic pressure on the plate. Apart from the plate equation itself other natural conditions of $\delta L = 0$ are the free edge conditions described by (2), and (3). Thus, using the variational principle means that the edge conditions are satisfied indirectly as part of the approximation.

If we now substitute the approximation for w and ϕ in (18) into the above and minimise (i.e. apply $\delta L = 0$) we obtain

$$\beta \mathbb{K} \vec{\mathbf{w}} + (1 - k\gamma) \mathbb{M} \vec{\mathbf{w}} = k \mathbb{M} \vec{\phi}, \quad (21)$$

where the stiffness matrix \mathbb{K} , is given by

$$\mathbb{K} = \int_{\Delta_0} \left[\frac{\partial^2 \vec{\chi}}{\partial x^2} \frac{\partial^2 \vec{\chi}^T}{\partial x^2} + \frac{\partial^2 \vec{\chi}}{\partial y^2} \frac{\partial^2 \vec{\chi}^T}{\partial y^2} \right] d\mathbf{x} \quad (22)$$

$$+ 2(1 - \nu) \frac{\partial^2 \vec{\chi}}{\partial x \partial y} \frac{\partial^2 \vec{\chi}^T}{\partial x \partial y} + \nu \frac{\partial^2 \vec{\chi}}{\partial x^2} \frac{\partial^2 \vec{\chi}^T}{\partial y^2} + \nu \frac{\partial^2 \vec{\chi}}{\partial y^2} \frac{\partial^2 \vec{\chi}^T}{\partial x^2} \Big] d\mathbf{x} \quad (23)$$

and the mass matrix \mathbb{M} is given by

$$\mathbb{M} = \int_{\Delta_0} \vec{\chi}(\mathbf{x}) \vec{\chi}^T(\mathbf{x}) d\mathbf{x}. \quad (24)$$

The integral equation (16) is transformed by substituting the approximations for w and ϕ given by (18) to obtain

$$\vec{\chi}^T(\mathbf{x}) \vec{\phi} = \vec{\chi}^T(\mathbf{x}) \vec{\phi}^{\text{in}} + \int_{\Delta_0} G_{\mathbf{P}}(\mathbf{x}; \boldsymbol{\xi}) \left[k \vec{\chi}^T(\boldsymbol{\xi}) \vec{\phi} - \vec{\chi}^T(\boldsymbol{\xi}) \vec{w} \right] d\boldsymbol{\xi} \quad (25)$$

(where where $\vec{\phi}^{\text{in}}$ is the representation of ϕ^{in} in the basis functions χ) and then multiplying this equation by $\vec{\chi}(\mathbf{x})$ and integrating over Δ_0 . This gives us

$$\mathbb{M} \vec{\phi} = \mathbb{M} \vec{\phi}^{\text{in}} + k \mathbb{G}_{\mathbf{P}} \vec{\phi} - \mathbb{G}_{\mathbf{P}} \vec{\mathbf{w}}, \quad (26)$$

where $\mathbb{G}_{\mathbf{P}}$, is given by

$$\mathbb{G}_{\mathbf{P}} = \int_{\Delta_0} \int_{\Delta_0} \vec{\chi}(\mathbf{x}) G_{\mathbf{P}}(\mathbf{x}, \boldsymbol{\xi}) \vec{\chi}^T(\mathbf{x}) d\mathbf{x} d\boldsymbol{\xi}. \quad (27)$$

We can use equation (19) to express the matrices \mathbb{K} , \mathbb{M} , and $\mathbb{G}_{\mathbf{P}}$ as

$$\begin{aligned} \mathbb{K} = & \sum_{d=1}^N [o]_d^T \left[\int_{\Delta_d} \left(\frac{\partial^2 \mathbf{N}_d^T}{\partial x^2} \frac{\partial^2 \mathbf{N}_d}{\partial x^2} \right) + \nu \left(\frac{\partial^2 \mathbf{N}_d^T}{\partial x^2} \frac{\partial^2 \mathbf{N}_d}{\partial y^2} + \frac{\partial^2 \mathbf{N}_d^T}{\partial y^2} \frac{\partial^2 \mathbf{N}_d}{\partial x^2} \right) \right. \\ & \left. + 2(1-\nu) \left(\frac{\partial^2 \mathbf{N}_d^T}{\partial x \partial y} \frac{\partial^2 \mathbf{N}_d}{\partial x \partial y} \right) + \left(\frac{\partial^2 \mathbf{N}_d^T}{\partial y^2} \frac{\partial^2 \mathbf{N}_d}{\partial y^2} \right) d\mathbf{x} \right] [o]_d, \quad (28) \end{aligned}$$

$$\mathbb{M} = \sum_{d=1}^N [o]_d^T \left[\int_{\Delta_d} \mathbf{N}_d^T(\mathbf{x}) \mathbf{N}_d(\mathbf{x}) d\mathbf{x} \right] [o]_d, \quad (29)$$

and

$$\mathbb{G}_{\mathbf{P}} = \sum_{e=1}^p \sum_{d=1}^p [o]_e^T \left[\int_{\Delta_e} \int_{\Delta_d} \mathbf{N}_e^T(\mathbf{x}) G_{\mathbf{P}}(\mathbf{x}, \boldsymbol{\xi}) \mathbf{N}_d(\boldsymbol{\xi}) d\mathbf{x} d\boldsymbol{\xi} \right] [o]_d. \quad (30)$$

These are the equations which are used to find to calculate the matrices \mathbb{K} , \mathbb{M} , and \mathbb{G} . The solution for \vec{w} and $\vec{\phi}$ is then found by solving equation (21) simultaneously with (26).

5. Accelerating the Convergence of the Periodic Green Function

The spatial representation of the far-field periodic Green's function equation (17) is slowly convergent, with terms decaying in magnitude like $O(n^{-1/2})$ and in this section we show how to accelerate the convergence. We begin with the asymptotic approximation of the three-dimensional Green function (15) far from the source point,

$$G(\mathbf{x}, 0; \boldsymbol{\xi}) \sim -\frac{ik}{2} H_0(k|\mathbf{x} - \boldsymbol{\xi}|), \quad \text{as } |\mathbf{x} - \boldsymbol{\xi}| \rightarrow \infty, \quad (31)$$

(Wehausen and Laitone, 1960) where $H_0 \equiv H_0^{(1)}$ is the Hankel function of the first kind of order zero (Abramowitz and Stegun, 1970). In (Linton, 1998) various methods were described in which the convergence of the periodic Green functions was improved. One such method, which suits the particular problem being considered here, involves writing the

periodic Green function as

$$G_{\mathbf{P}}(\mathbf{x}; \boldsymbol{\xi}) = \sum_{m=-\infty}^{\infty} \left[G(\mathbf{x}; \boldsymbol{\xi} + (0, ml)) + \frac{ik}{2} H_0\left(k\sqrt{(X+cl)^2 + Y_m^2}\right) \right] e^{im\sigma l} \\ - \sum_{m=-\infty}^{\infty} \frac{ik}{2} H_0\left(k\sqrt{(X+cl)^2 + Y_m^2}\right) e^{im\sigma l} \quad (32)$$

where c is a numerical smoothing parameter, introduced to avoid the singularity at $\mathbf{x} = \boldsymbol{\xi}$ in the Hankel function, and

$$X = x - \xi, \quad \text{and} \quad Y_m = (y - \eta) - m.$$

The first term in (32) is now much more rapidly convergent than in its original form and we use the fact that second slowly convergent sum in (32) can be transformed to

$$-\frac{i}{l} \sum_{m=-\infty}^{\infty} \frac{e^{ik\mu_m|X+c|} e^{i\sigma_m Y_0}}{\mu_m} \quad (33)$$

(Linton, 1998; Jorgenson and Mittra, 1990; Singh et al., 1990) where $\sigma_m = \sigma + 2m\pi/l$ and

$$\mu_m = \left[1 - \left(\frac{\sigma_m}{k} \right)^2 \right]^{\frac{1}{2}}.$$

Combining equations (32) and (33) we obtain the accelerated version of the periodic Green's function

$$G_{\mathbf{P}}(\mathbf{x}; \boldsymbol{\xi}) = \sum_{m=-\infty}^{\infty} \left[G(\mathbf{x}; \boldsymbol{\xi} + (0, ml)) + \frac{ik}{2} H_0\left(k\sqrt{(X+cl)^2 + Y_m^2}\right) \right] e^{im\sigma l} \\ - \frac{i}{l} \sum_{m=-\infty}^{\infty} \frac{e^{ik\mu_m|X+c|} e^{i\sigma_m Y_0}}{\mu_m}. \quad (34)$$

Note that some special combinations of wavelength λ and angle of incidence θ cause the periodic Green's function to diverge ((Jorgenson and Mittra, 1990), (Scott, 1998)). This singularity is closely related to the diffracted waves and will be explained shortly.

6. The scattered waves

We begin with the accelerated periodic Green function, equation (34) setting $c = 0$ and considering the case when X is large (positive or

negative). We also note that for m sufficiently small or large the U_m will be negative and the corresponding terms will decay. Therefore

$$G_{\mathbf{P}}(\mathbf{x}; \boldsymbol{\xi}) \sim -\frac{i}{l} \sum_{m=-M}^N \frac{e^{ik\mu_m|X|} e^{i\sigma_m Y_0}}{\mu_m}, \quad \text{as } X \rightarrow \pm\infty \quad (35)$$

where the integers M and N satisfy the following inequalities

$$\left. \begin{array}{l} \sigma_{-M-1} < -k < \sigma_{-M}, \\ \sigma_N < k < \sigma_{N+1}. \end{array} \right\} \quad (36)$$

Equations (36) can be written as

$$\frac{l}{2\pi} (\sigma + k - 2\pi) < M < \frac{l}{2\pi} (\sigma + k), \quad (37)$$

and

$$\frac{l}{2\pi} (k - \sigma) > N > \frac{l}{2\pi} (k - \sigma - 2\pi) \quad (38)$$

(Linton, 1998). It is obvious that $G_{\mathbf{P}}$ will diverge if $\sigma_m = \pm k$; these values correspond to cut-off frequencies which are an expected feature of periodic structures.

6.1. THE DIFFRACTED WAVES

The diffracted waves are the plane waves which are observed as $x \rightarrow \pm\infty$. Their amplitude and form are obtained by substituting the limit of the periodic Green function (35) as $x \rightarrow \pm\infty$ into the boundary integral equation for the potential (16). This gives us

$$\lim_{x \rightarrow \pm\infty} \phi^s(\mathbf{x}, 0) = -\frac{i}{l} \sum_{m=-M}^N \int_{\Delta_0} \frac{e^{ik\mu_m|X|} e^{i\sigma_m Y_0}}{\mu_m} [k\phi(\boldsymbol{\xi}, 0) - w(\boldsymbol{\xi})] d\boldsymbol{\xi}, \quad (39)$$

where $\phi^s = \phi - \phi^{\text{in}}$ is the scattered wave and is composed of a finite number of plane waves. For negative x we write

$$\lim_{x \rightarrow -\infty} \phi^s(\mathbf{x}, 0) = A_m^- e^{ik\mu_m x} e^{i\sigma_m y}, \quad (40)$$

where the amplitudes A_m^- are identified from (39) as

$$A_m^- = -\frac{i}{\mu_m l} \int_{\Delta_0} e^{ik\mu_m \xi} e^{-i\sigma_m \eta} [k\phi(\boldsymbol{\xi}) - w(\boldsymbol{\xi})] d\boldsymbol{\xi}. \quad (41)$$

Likewise as $x \rightarrow \infty$ it is given by

$$\lim_{x \rightarrow \infty} \phi^s(\mathbf{x}, 0) = A_m^+ e^{-ik\mu_m x} e^{i\sigma_m y}, \quad (42)$$

where A_m^+ are

$$A_m^+ = -\frac{i}{\mu_m l} \int_{\Delta_0} e^{-ik\mu_m \xi} e^{-i\sigma_m \eta} [k\phi(\boldsymbol{\xi}, 0) - w(\boldsymbol{\xi})] d\boldsymbol{\xi}. \quad (43)$$

The diffracted waves propagate at various angles with respect to the normal direction of the array. The angles of diffraction, ψ_m^\pm , are given by

$$\psi_m^\pm = \tan^{-1} \left(\frac{\sigma_m}{\pm k\mu_m} \right). \quad (44)$$

Notice that for $m = 0$ we have

$$\psi_0^\pm = \pm\theta, \quad (45)$$

where θ is the incident angle. This is exactly as expected since we should always have a transmitted wave which travels in the same direction as the incident wave and a reflected wave which travels in the negative incident angle direction.

6.2. THE FUNDAMENTAL REFLECTED AND TRANSMITTED WAVES

We need to be slightly careful when we determine the wave of order zero at $x \rightarrow \infty$ because we have to include the incident wave. There is always at least one set of propagating waves corresponding to $m = 0$ which correspond to simple reflection and transmission. The coefficient, R , for the fundamental reflected wave for the $m = 0$ mode is given by

$$R = A_0^- = -\frac{i}{\mu_0 l} \int_{\Delta_0} e^{ik(\xi \cos \theta - \eta \sin \theta)} [k\phi(\boldsymbol{\xi}, 0) - w(\boldsymbol{\xi})] d\boldsymbol{\xi}. \quad (46)$$

The coefficient, T , for the fundamental transmitted wave for the $m = 0$ mode is given by

$$T = 1 + A_0^+ = 1 - \frac{i}{\mu_0 l} \int_{\Delta_0} e^{-ik(\xi \cos \theta + \eta \sin \theta)} [k\phi(\boldsymbol{\xi}, 0) - w(\boldsymbol{\xi})] d\boldsymbol{\xi}. \quad (47)$$

6.3. CONSERVATION OF ENERGY

The diffracted wave, taking into account the correction for T , must satisfy the energy flux equation. This simply says that the energy of the incoming wave must be equal to the energy of the outgoing waves. This gives us

$$\cos \theta = (|R|^2 + |T|^2) \cos \theta + \sum_{\substack{m=-M \\ m \neq 0}}^N (|A_m^-|^2 \cos \psi_m^- + |A_m^+|^2 \cos \psi_m^+). \quad (48)$$

Table I. The coefficients A_m^\pm for the case of a dock of geometry 1 with $\lambda = 4$, $l = 6$ and $\theta = \pi/6$.

| m | A_m^- | A_m^+ |
|-----|-------------------|-------------------|
| -2 | $-0.214 - 0.042i$ | $0.232 + 0.023i$ |
| -1 | $0.266 - 0.268i$ | $-0.185 + 0.349i$ |
| 0 | $0.631 - 0.210i$ | $-0.702 - 0.141i$ |

The energy balance equation (48) can be used as an accuracy check on the numerical results.

7. Results

We tested the convergence of our accelerated version of the Green function and we use $c = 0.005$ and 44 terms in the spatial representation and 46 terms in the spectral representation of the accelerated $G_{\mathbf{P}}$ (equation (34)) in all our subsequent calculations. We consider four geometries for the plates which are shown in figure 2.

7.1. SCATTERING FROM A DOCK

Aside from the energy balance equation or wide spacing, it is difficult to compare our results to establish their validity. However, there is one case in which we can make comparisons. If we consider the case when we have the dock boundary condition under the plate (so that $w = 0$) and the plates are square and joined then the problem reduces to a two dimensional dock problem which is discussed extensively in (Linton and McIver, 2001). To impose the condition of a dock we simply solve equation (26) setting \vec{w} to zero (we do not require equation (21)), choosing plate geometry 1 and setting the plate separation to $l = 4$.

Figure 3 show the reflection and transmission coefficients for a plate of geometry 1 with the plate separation $l = 4$ and the dock boundary condition (crosses) and the solution to the two-dimensional dock problem using the method of (Linton and McIver, 2001) (solid and dashed lines). As expected the results agree. Table I shows the values of the coefficient A_m^\pm for a dock of geometry 1 with $\lambda = 4$, $l = 6$ and $\theta = \pi/6$. These results are given to assist in numerical comparisons.

Table II. The coefficients A_m^\pm for the case of an elastic plate of geometry 1 with $\beta = 0.1$, $\gamma = 0$, $\lambda = 4$, $l = 6$ and $\theta = \pi/6$.

| m | A_m^- | A_m^+ |
|-----|-------------------|-------------------|
| -2 | $0.001 + 0.014i$ | $-0.040 - 0.016i$ |
| -1 | $-0.016 - 0.008i$ | $-0.070 - 0.099i$ |
| 0 | $-0.058 - 0.072i$ | $-0.209 - 0.582i$ |

7.2. SCATTERING FROM ELASTIC PLATES

We begin with a short table of numerical results. Table (II) is equivalent to Table I except that the plate is now elastic with $\beta = 0.1$ and $\gamma = 0$. As expected the reflected energy is less because the waves can propagate under the elastic plates. Figures 4 and 5 show the amplitudes of the diffracted waves due to the array as a function of the incident angle for plates of geometry one and two respectively with $\beta = 0.1$, $\gamma = 0$, $k = \pi/2$, and $l = 6$. There are 3 pairs of diffracted waves (including the reflected-transmitted pair) for any angle. $G_{\mathbf{P}}$ diverges if $\sigma_n = \pm k$ which for our values of l and k means that $\theta = \pm 0.3398$. As θ moves across these points one of the diffracted waves disappears (at $\pm\pi/2$) and another appears (at $\mp\pi/2$). In the plots we have plotted A_{-2}^\pm and A_1^\pm with the same line style and also A_{-1}^\pm and A_2^\pm since they represent diffracted waves which appear and disappear together. Interestingly the result of doing this is to produce smooth curves for $-\pi/2 < \theta < \pi/2$.

Figures 6. to 9 show the real part of the displacement for five plates (Δ_j , $j = -2, -1, 0, 1, 2$) of the array for plates of geometry one to four respectively, with $\beta = 0.1$, $\gamma = 0$, and $l = 6$. The angle of incidence is $\theta = \pi/6$. We consider two values of the wavenumber, $k = \pi/2$ (a) and $k = \pi/4$ (b). The complex response of the elastic plates is apparent in these figures as is the coupling between the the water and the plate.

8. Summary

Motivated by the problem of modelling wave propagation in the marginal ice zone we have presented a solution to the problem of wave scattering by an infinite array of floating elastic plates. The solution method is similar to that used to solve for a single plate except that the periodic Green function must be used. We have shown how the calculation of the periodic Green function can be accelerated and how the diffracted wave far from the array can be calculated. We have checked our numerical

calculations for energy balance and against the limiting case when the plates are rigid and joined where the solution reduces to that of a rigid dock. We have also presented solutions for a range of elastic plate geometries.

References

- Abramowitz, M. and I. A. Stegun: 1970, *Handbook of Mathematical Functions*. Dover.
- Chou, T.: 1998, 'Band structure of surface flexural-gravity waves along periodic interfaces'. *J. Fluid Mech.* **369**, 333–350.
- de Veubeke, F.: 1979, *A course in elasticity*. Springer-Verlag.
- Evans, R. P. . D. V.: 1995, 'Wave Scattering by Periodic Arrays of Breakwaters'. *Wave Motion* **23**, 95–120.
- Evans, R. P. . D. V.: 1999, 'Rayleigh-Bloch surface waves along periodic grating and their connection with trapped modes in waveguides'. *J. Fluid Mech.* **386**, 233–258.
- Fernyhough, M. and D. V. Evans: 1995, 'Scattering by a Periodic Array of Rectangular Blocks'. *J. Fluid Mech.* **305**, 263–279.
- Hildebrand, F. B.: 1965, *Methods of Applied Mathematics*. Prentice-Hall, 2nd edition.
- Jorgenson, R. E. and R. Mittra: 1990, 'Efficient Calculation of the Free-Space Periodic Green's Function'. *IEEE Transaction on Antennas and Propagation* **38**, 633–642.
- Kashiwagi, M.: 2000, 'Research on Hydroelastic Response of VLFS: Recent Progress and Future Work'. *Int. Journal of Offshore and Polar Engineering* **10**(2), 81–90.
- Kim, W. D.: 1965, 'On the harmonic oscillations of a rigid body on a free surface'. *J. Fluid Mech.* **21**, 427–451.
- Linton, C. M.: 1998, 'The Green's Function for the Two-Dimensional Helmholtz Equation in Periodic Domains'. *J. Eng. Maths* **33**, 377–402.
- Linton, C. M. and D. V. Evans: 1993, 'The interaction of waves with a row of circular cylinders'. *J. Fluid Mech* **251**, 687–708.
- Linton, C. M. and P. McIver: 2001, *Handbook of Mathematical Techniques for Wave / Structure Interactions*. Chapman & Hall /CRC.
- Maniar, H. and J. N. Newman: 1997, 'Wave Diffraction by Long Arrays of Cylinders'. *J. Fluid Mech* **339**, 309–330.
- Meylan, M. H.: 2001, 'A Variation Equation for the Wave Forcing of Floating Thin Plates'. *J. of Applied Ocean Res.* **23**(4), 195–206.
- Meylan, M. H.: 2002, 'The Wave Response of Ice Floes of Arbitrary Geometry'. *J. of Geophysical Research - Oceans* **107**(C6).
- Meylan, M. H. and V. A. Squire: 1996, 'Response of a Circular Ice Floe to Ocean Waves'. *J. of Geophysical Research* **101**(C4), 8869–8884.
- Petyt, M.: 1990, *Introduction to Finite Element Vibration Analysis*. Cambridge University Press.
- Porter, D. and R. Porter: 2004, 'Approximations to Wave Scattering by an Ice Sheet of Variable Thickness over Undulating Bed Topography'. *J. Fluid Mech.* **509**, 145–179.
- Scott, C.: 1998, *Introduction to Optics and Optical Imaging*. IEEE Press.
- Singh, S., W. Richards, J. R. Zinecker, and D. R. Wilton: 1990, 'Accelerating the Convergence of Series Representing the Free-Surface Periodic Green's Function'. *IEEE Transaction on Antennas and Propagation* **38**(12), 1958–1962.
- Squire, V. A., J. P. Duggan, P. Wadhams, P. J. Rottier, and A. J. Liu: 1995, 'Of Ocean Waves and Sea Ice'. *Annu. Rev. Fluid Mech.* **27**, 115–168.
- Tayler, A. B.: 1986, *Mathematical Models in Applied Mathematics*. Clarendon Press.
- Timoshenko, S. and S. Woinowsky-Krieger: 1959, *Theory of plates and shells*. McGraw-Hill.

- Twersky, V.: 1952, 'Multiple scattering or radiation by an arbitrary configuration of parallel cylinders.'. *J. Acoust. Soc. Am.* **24**, 42–46.
- Wang, S. D. and M. H. Meylan: 2004, 'A higher order coupled boundary element and finite element method for the wave forcing of a floating thin plate'. *J. of Fluids and Structures* **19**(4), 557–572.
- Watanabe, E., T. Utsunomiya, and C. Wang: 2004, 'Hydroelastic analysis of pontoon-type VLFS: a literature survey'. *Eng. Struct.* **26**(2), 245–256.
- Wehausen, J. and E. Laitone: 1960, 'Surface Waves'. In: S. Flügge and C. Truesdell (eds.): *Fluid Dynamics III*, Vol. 9 of *Handbuch der Physik*. Springer Verlag, Chapt. 3, pp. 446–778.

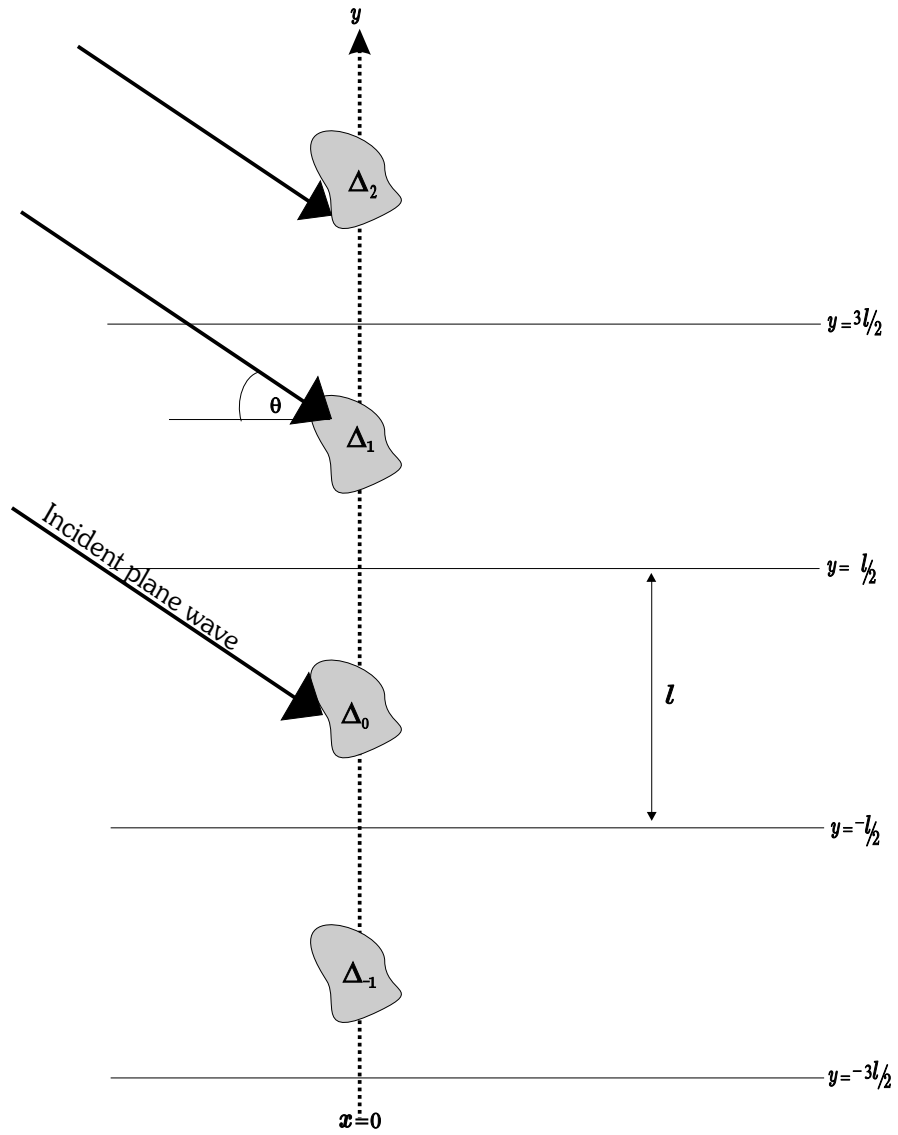


Figure 1. A schematic diagram of the periodic array of floating elastic plates.

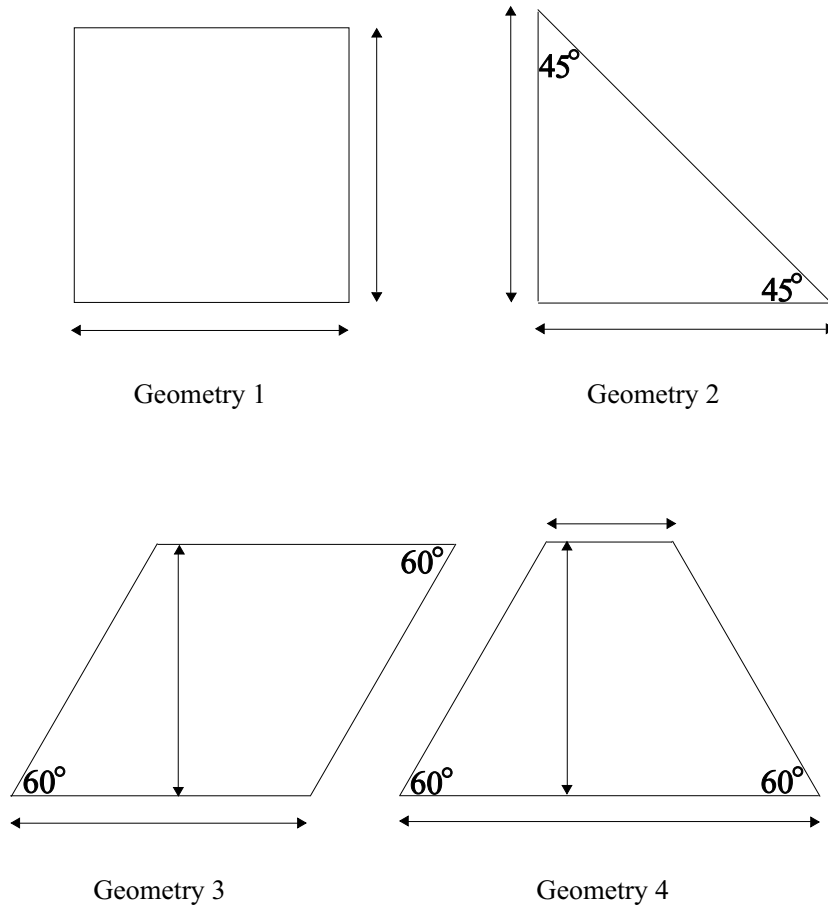


Figure 2. Diagram of the four plate geometries for which we will calculate solutions.

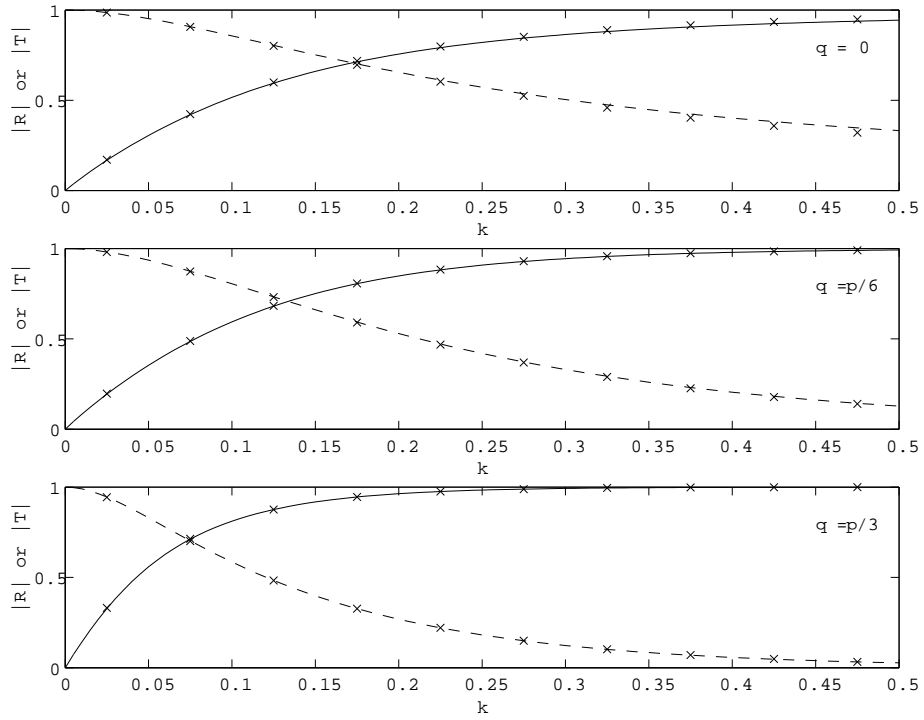


Figure 3. The reflection coefficient R (solid line) and the transmission coefficient T (dashed line) as a function of k for a two-dimensional dock of length 4 for the incident angles shown. The crosses are the same problem solved using the three-dimensional array code with the dock boundary condition and using plates of geometry 1 with $l = 4$.

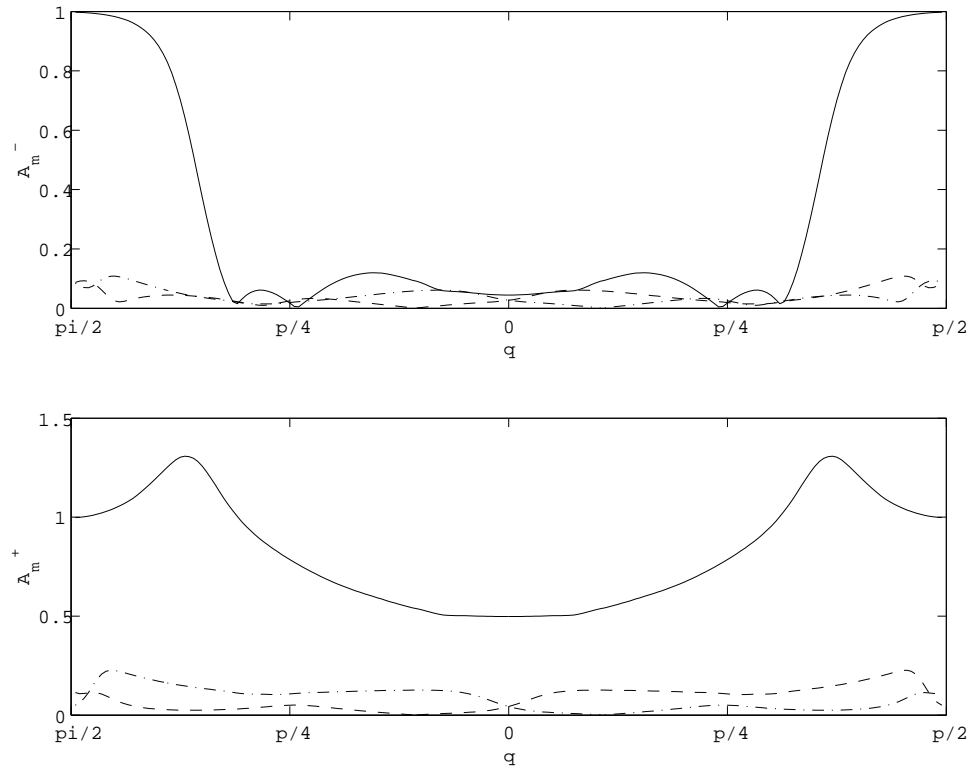


Figure 4. The diffracted waves A_m^\pm for a periodic array of geometry one plates with $k = \pi/2$, $l = 6$, $\beta = 0.1$, $\gamma = 0$, and $l = 6$. The solid line is A_0^\pm , the chained line is A_{-2}^\pm and A_1^\pm and the dashed line is A_{-1}^\pm and A_2^\pm .

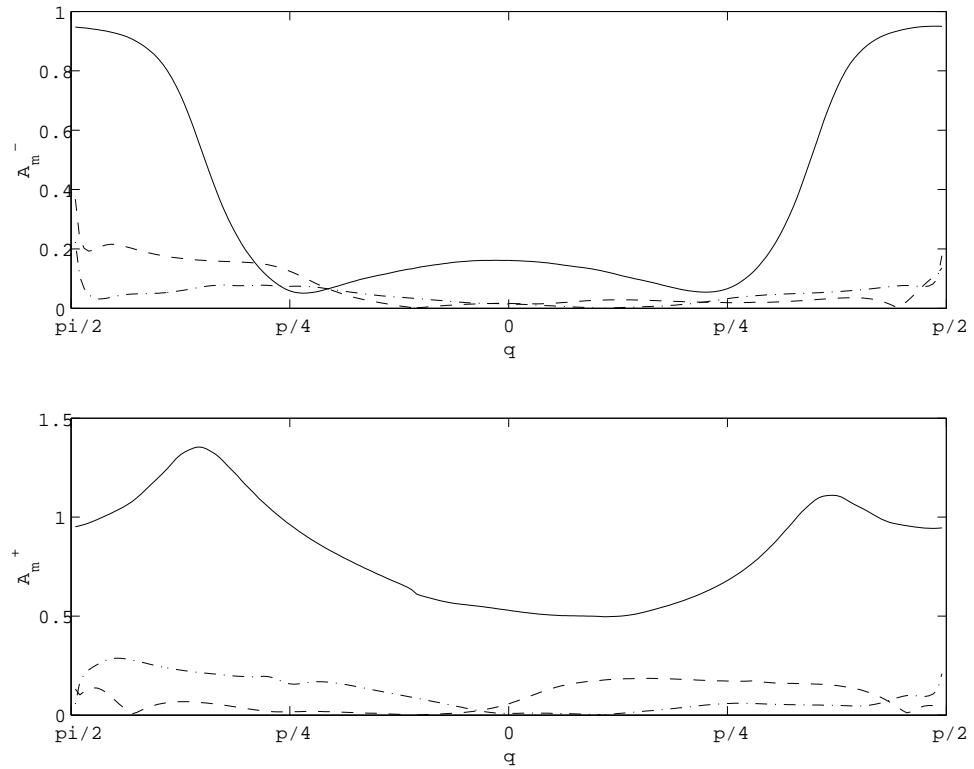


Figure 5. As for figure 4 except that the pate has geometry 2.

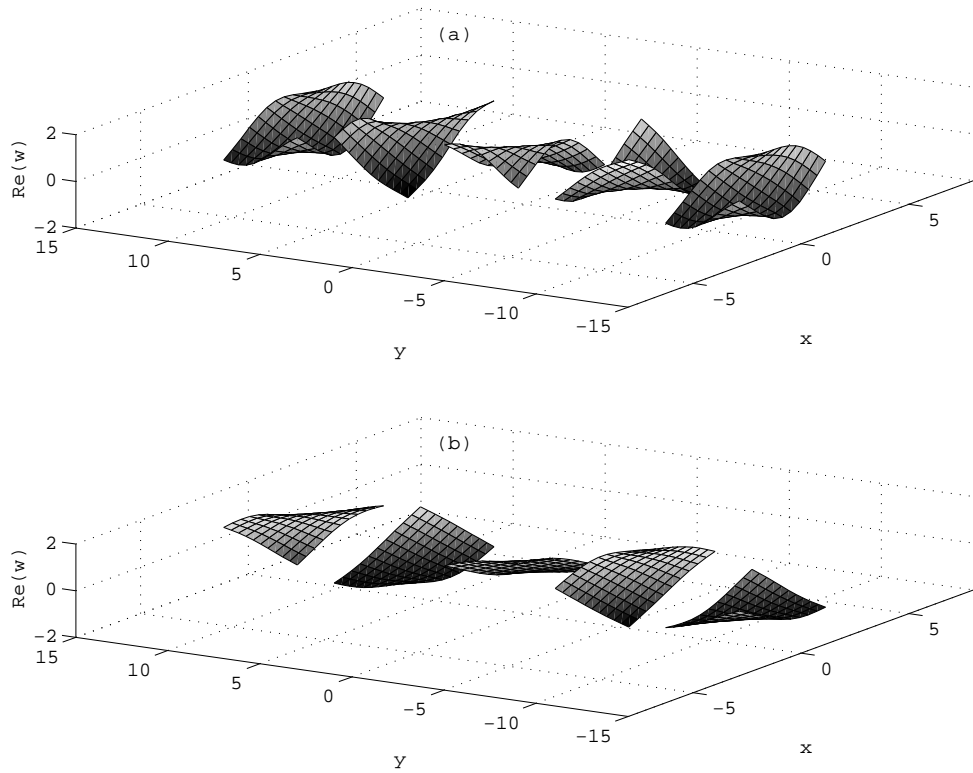


Figure 6. The real part of the displacement w for five plates of geometry one which are part of a periodic array, $l = 6$, $\theta = \pi/6$, $\beta = 0.1$, $\gamma = 0$ and (a) $k = \pi/2$ and (b) $k = \pi/4 = 8$.

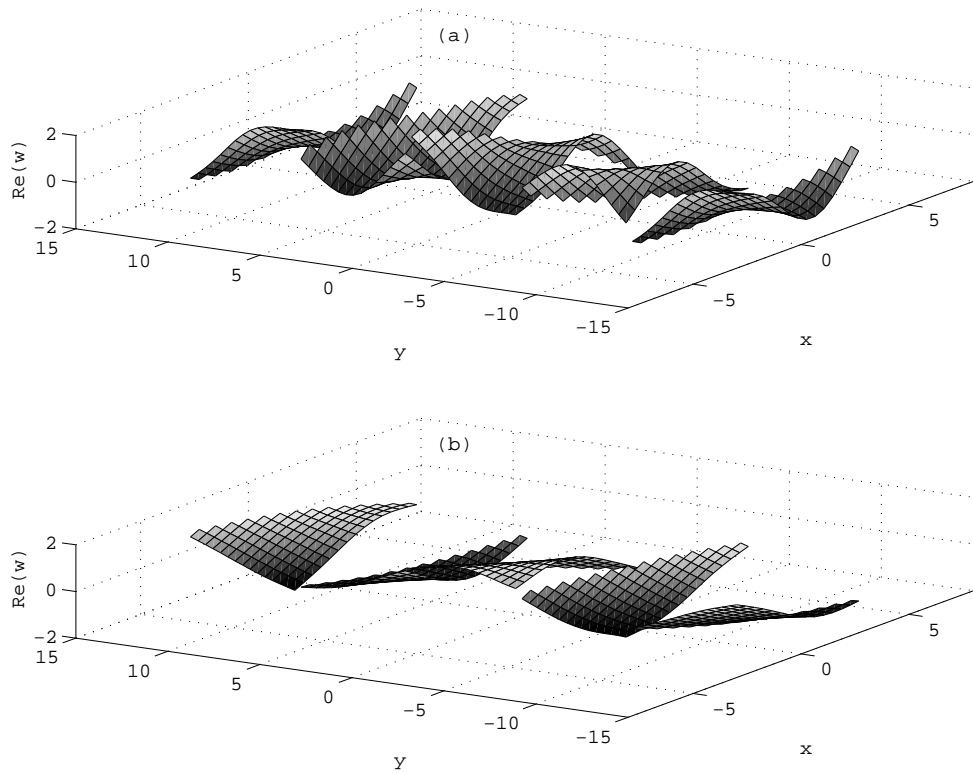


Figure 7. As for figure 6 except that the plate is of geometry two.

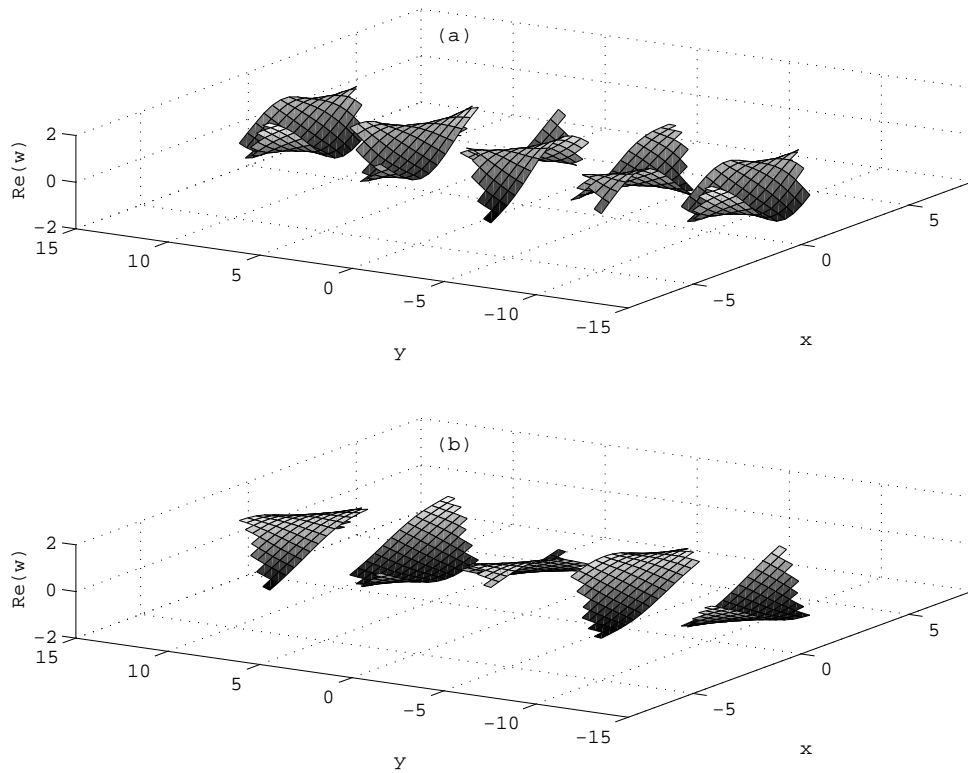


Figure 8. As for figure 6 except that the plate is of geometry three.

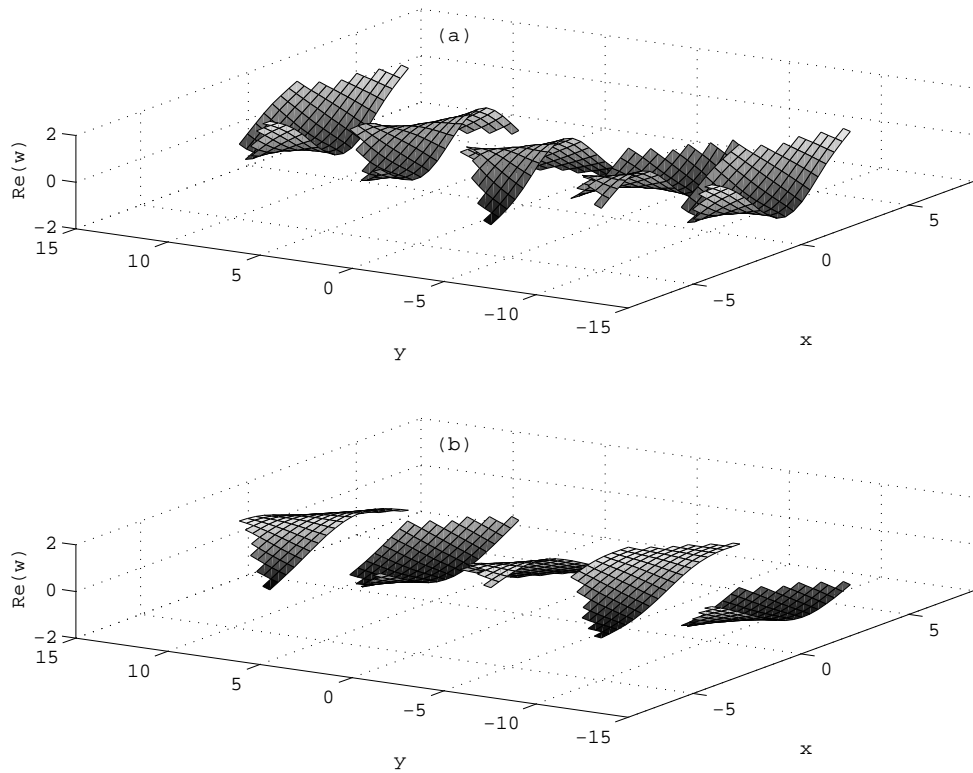


Figure 9. As for figure 6 except that the plate is of geometry four.